

New lithium-ion conductors based on the NASICON structure†

Venkataraman Thangadurai, Ashok K. Shukla and Jagannatha Gopalakrishnan*

Solid State and Structural Chemistry Unit, Indian Institute of Science, Bangalore 560 012, India.
E-mail: gopal@sscu.iisc.ernet.in

Received 8th September 1998, Accepted 22nd December 1998

Lithium-ion conduction in mixed-metal phosphates, $\text{LiM}^{\text{V}}\text{M}^{\text{III}}(\text{PO}_4)_3$ [$\text{M}^{\text{V}} = \text{Nb, Ta}$; $\text{M}^{\text{III}} = \text{Al, Cr, Fe}$], possessing the rhombohedral ($R\bar{3}c$) NASICON structure has been investigated. Among the phosphates investigated, $\text{LiTaAl}(\text{PO}_4)_3$ exhibits the highest conductivity, $\sigma \approx 1.0 \times 10^{-2} \text{ S cm}^{-1}$ at 350°C ($E_a = 0.47 \text{ eV}$), comparable to the conductivity of $\text{LiTi}_2(\text{PO}_4)_3$. Unlike $\text{LiTi}_2(\text{PO}_4)_3$ which contains lithium-reducible Ti^{IV} , $\text{LiTaAl}(\text{PO}_4)_3$ contains stable Ta^{V} and Al^{III} oxidation states and hence deserves further attention towards tailoring new lithium-ion conductors for application as electrolytes in solid state lithium batteries.

At present, there is a great interest to develop solid lithium-ion conductors for use as electrolytes in all-solid-state-lithium batteries.¹ Availability of a suitable solid electrolyte material that could replace the currently used liquid electrolytes in lithium batteries would greatly contribute to the development of lithium battery technology by enabling fabrication of flexible, compact and leak-proof batteries of desired geometry.¹ Two approaches are pursued for this purpose. One approach² is to render liquid polymer electrolytes [such as polyethylene oxide (PEO)-lithium salt complexes] into solid composites by adding solid plasticizers (such as TiO_2 or Al_2O_3) without loss of conducting properties. The other approach is to synthesise lithium-containing solid compounds possessing the desired conducting properties.³

Among the several families of inorganic solids exhibiting lithium-ion conduction,³ framework oxides based on the NASICON structure (Fig. 1) are of special interest, because materials exhibiting high conductivities combined with low activation energies have been reported for this structure.⁴ For example, the titanium-aluminium system,⁵ $\text{Li}_{1+x}\text{Ti}_{2-x}\text{Al}_x(\text{PO}_4)_3$, exhibits a high conductivity ($7.0 \times 10^{-4} \text{ S cm}$ at 25°C) and a low activation energy ($E_a = 0.2\text{--}0.3 \text{ eV}$) for $x = 0.3$. Despite these attractive features, there are several materials-problems to be overcome before a lithium-ion conductor based on the NASICON framework could find application as electrolyte material. For instance, it is not clear whether the high conductivity of $\text{Li}_{1+x}\text{Ti}_{2-x}\text{Al}_x(\text{PO}_4)_3$ and other such trivalent metal-substituted systems are intrinsic to the structure or due to formation of secondary phases that favour sintering and eliminate grain-boundary resistance.³ More importantly, for electrolyte application, the Ti^{IV} in the material should be replaced by other metal ions that would not undergo reduction by lithium. Towards this end, we examined lithium-ion conduction of mixed-metal NASICON-phases of the formula,⁶ $\text{LiM}^{\text{V}}\text{M}^{\text{III}}(\text{PO}_4)_3$, where $\text{M}^{\text{V}} = \text{Nb, Ta}$; $\text{M}^{\text{III}} = \text{Al, Cr, Fe}$. We believed that once we obtain a stoichiometric NASICON-phase possessing intrinsic conducting properties similar to $\text{LiTi}_2(\text{PO}_4)_3$ but without Ti^{IV} , extraneous factors such as sinterability, grain boundary resistance, etc., could be tailored by appropriate means to obtain a favourable conducting material for application. Our results, which are reported in this paper, reveal that, among the phases investigated, $\text{LiTaAl}(\text{PO}_4)_3$ exhibiting a total (bulk + grain boundary) conductivity of ca. $6.5 \times 10^{-7} \text{ S cm}^{-1}$ at 30°C and ca. $1.0 \times 10^{-2} \text{ S cm}^{-1}$ at 350°C deserves further attention. It must

be mentioned that Nb- and Ta-containing NASICONs, $\text{Li}_{1-x}\text{M}^{\text{IV}}_{2-x}\text{M}^{\text{V}}_x(\text{PO}_4)_3$, have been investigated for their lithium-ion conductivity.⁷

Experimental

$\text{LiM}^{\text{V}}\text{M}^{\text{III}}(\text{PO}_4)_3$ phosphates, where $\text{M}^{\text{V}} = \text{Nb, Ta}$; $\text{M}^{\text{III}} = \text{Al, Cr, Fe}$, were prepared by reacting stoichiometric mixtures of Li_2CO_3 , $\text{M}^{\text{V}}_2\text{O}_5$, Al_2O_3 , Cr_2O_3 and/or $\text{FeC}_2\text{O}_4 \cdot 2\text{H}_2\text{O}$ at 800°C for 24 h in air as described in the literature.⁶ The phosphates were characterised by powder X-ray diffraction (XRD) (Siemens D50005 powder diffractometer, $\text{Cu-K}\alpha$ radiation). Lattice parameters were derived from least-squares refinement of powder X-ray diffraction data (Fig. 2). Lithium-ion conductivities were measured on sintered pellets (sintered at 800°C for 24 h) coated with gold paste (cured at 600°C for 6 h) using a HP4194A Impedance/Gain-Phase Analyzer over the frequency range 100 Hz–15 MHz in the temperature range $30\text{--}600^\circ\text{C}$ in air. For each sample, measurement was made for both heating and cooling cycles. Samples were equilibrated at constant temperature for about 1 h prior to each impedance measurement. Typical impedance plots are shown in Fig. 3. We see that, while the impedance plots [Fig. 3(a) and (b)] for

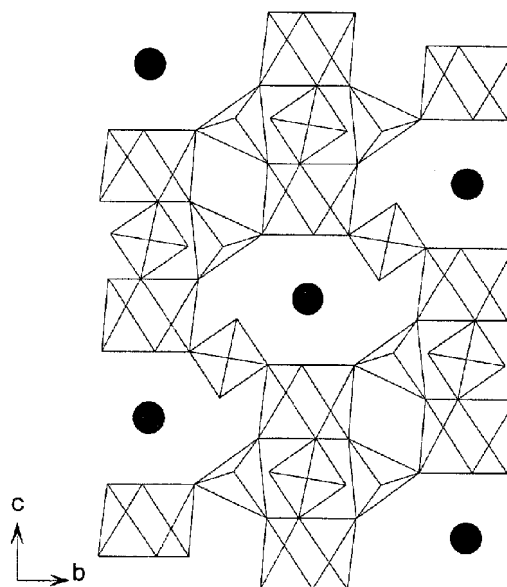


Fig. 1 $\text{LiM}^{\text{IV}}_2(\text{PO}_4)_3$ —NASICON structure showing the positions of Li atoms within the $\text{M}^{\text{IV}}_2(\text{PO}_4)_3$ framework.

†Contribution No. 1344 from the Solid State and Structural Chemistry Unit.

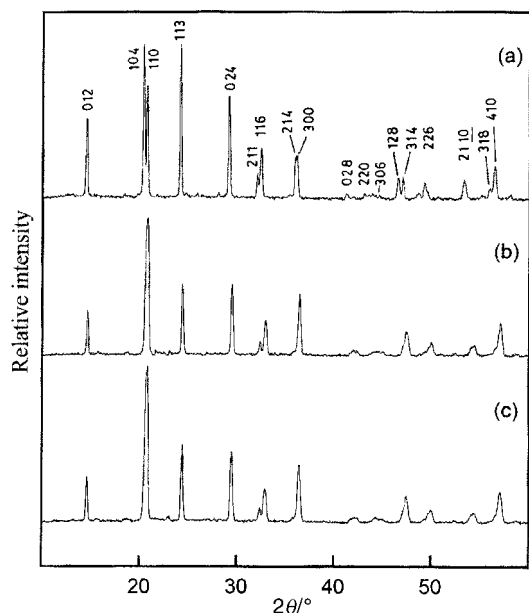


Fig. 2 Powder XRD patterns of (a) $\text{LiNbFe}(\text{PO}_4)_3$, (b) $\text{LiTaAl}(\text{PO}_4)_3$ and (c) $\text{Li}_{1.2}\text{Ta}_{0.9}\text{Al}_{1.1}(\text{PO}_4)_3$.

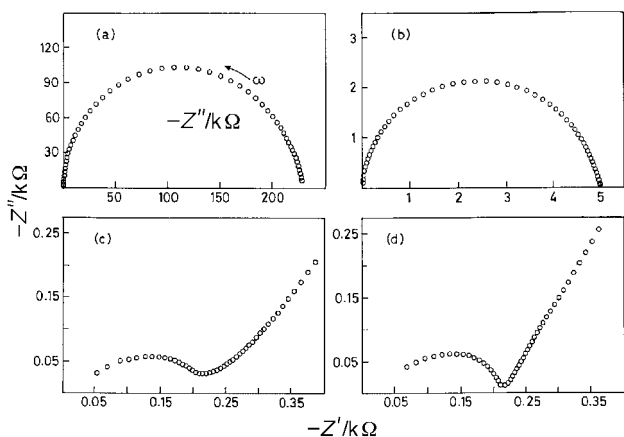


Fig. 3 Typical impedance plots of (a) $\text{LiNbFe}(\text{PO}_4)_3$, (b) $\text{LiTaFe}(\text{PO}_4)_3$, (c) $\text{LiTaAl}(\text{PO}_4)_3$ and (d) $\text{Li}_{1.2}\text{Ta}_{0.9}\text{Al}_{1.1}(\text{PO}_4)_3$ at $300\text{ }^\circ\text{C}$.

low-conducting samples, $\text{LiNbFe}(\text{PO}_4)_3$ and $\text{LiTaFe}(\text{PO}_4)_3$, are neat semicircles, the corresponding plots [Fig. 3(c) and (d)] for the higher conducting samples, $\text{LiTaAl}(\text{PO}_4)_3$ and $\text{Li}_{1.2}\text{Ta}_{0.9}\text{Al}_{1.1}(\text{PO}_4)_3$, show a spike on the low-frequency side due to electrode polarisation. Similar behaviour has been reported for other lithium-ion conductors.^{8,9} Since it was not possible to separate bulk and grain boundary contributions to the total conductivity, we obtained the total ionic conductivity

Table 1 Chemical composition, lattice parameters and total ionic conductivity data for NASICON-type phosphates $\text{LiM}^{\text{V}}\text{M}^{\text{III}}(\text{PO}_4)_3$ ($\text{M}^{\text{V}} = \text{Nb, Ta}$; $\text{M}^{\text{III}} = \text{Al, Cr, Fe}$)

Composition	Lattice parameters			$\sigma_{30^\circ\text{C}}/\text{S cm}^{-1}$	$\sigma_{350^\circ\text{C}}/\text{S cm}^{-1}$	E_a/eV
	$a_h/\text{Å}$	$c_h/\text{Å}$	$V/\text{Å}^3$			
$\text{LiNbFe}(\text{PO}_4)_3$	8.593(3)	21.715(8)	1388	$< 10^{-8}$	6.6×10^{-6}	0.85 (210–600 °C)
$\text{LiTaAl}(\text{PO}_4)_3$	8.542(6)	20.815(5)	1315	6.5×10^{-7}	1.0×10^{-2}	0.47 (30–250 °C)
$\text{LiTaCr}(\text{PO}_4)_3$	8.535(6)	21.551(8)	1360	$< 10^{-7}$	3.7×10^{-4}	0.49 (80–300 °C)
$\text{LiTaFe}(\text{PO}_4)_3$	8.608(6)	21.753(6)	1395	$< 10^{-7}$	3.0×10^{-4}	0.86 (150–350 °C)
$\text{Li}_{1.2}\text{Ta}_{0.9}\text{Al}_{1.1}(\text{PO}_4)_3$	8.513(4)	21.229(5)	1332	6.5×10^{-7}	1.2×10^{-2}	0.51 (30–250 °C)
$\text{LiTi}_2(\text{PO}_4)_3^a$	8.512	20.858	1310	2.0×10^{-6}	6.3×10^{-3}	0.30 (30–200 °C)
$\text{LiZr}_2(\text{PO}_4)_3^b$	8.850	22.240	1508	3.2×10^{-10}	5.0×10^{-3}	0.43 (300–400 °C)

^aData taken from ref. 13 and 14. ^bThe high temperature rhombohedral cell parameters are given. At low-temperatures, $\text{LiZr}_2(\text{PO}_4)_3$ has a monoclinic cell with $a = 15.299(1)$, $b = 8.940(1)$, $c = 8.612(2)$ Å, $\beta = 125.98(2)^\circ$, $V = 976 \text{ Å}^3$ (ref. 15).

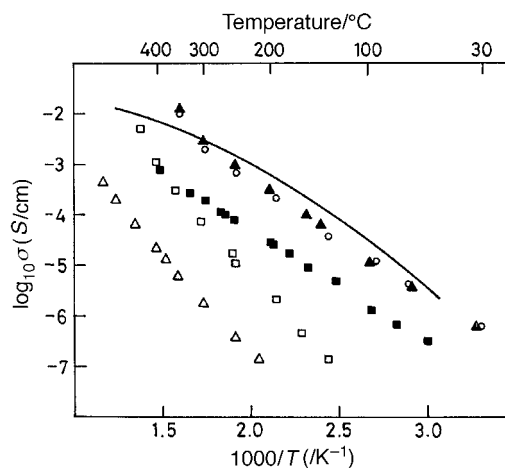


Fig. 4 Arrhenius plots for total lithium-ion conduction of $\text{LiNbFe}(\text{PO}_4)_3$ (Δ), $\text{LiTaAl}(\text{PO}_4)_3$ (\circ), $\text{LiTaCr}(\text{PO}_4)_3$ (\blacksquare), $\text{LiTaFe}(\text{PO}_4)_3$ (\square), and $\text{Li}_{1.2}\text{Ta}_{0.9}\text{Al}_{1.1}(\text{PO}_4)_3$ (\blacktriangle). For comparison, the corresponding data for $\text{LiTi}_2(\text{PO}_4)_3$ are also shown ($-$) (from ref. 14).

uniformly for all the samples, from the low frequency intercept of the impedance plots.

Results and discussion

In Table 1, we list the compositions of $\text{LiM}^{\text{V}}\text{M}^{\text{III}}(\text{PO}_4)_3$ ($\text{M}^{\text{V}} = \text{Nb, Ta}$; $\text{M}^{\text{III}} = \text{Al, Cr, Fe}$) phosphates, their lattice parameters and conductivity data. For comparison, we also give the corresponding data for $\text{LiM}^{\text{IV}}_2(\text{PO}_4)_3$ for $\text{M}^{\text{IV}} = \text{Ti}$ and Zr . All the $\text{LiM}^{\text{V}}\text{M}^{\text{III}}(\text{PO}_4)_3$ phosphates investigated by us crystallize in the rhombohedral ($R3c$) NASICON structure (Fig. 1)^{6,10} similar to $\text{LiM}^{\text{IV}}_2(\text{PO}_4)_3$.¹¹ In this structure, lithium atoms occupy the A_1 (6b) sites within the $M_2(\text{PO}_4)_3$ framework, the other possible A_2 (18e) sites being empty. Since we do not see evidence for a superstructure in the XRD patterns (Fig. 2) of $\text{LiM}^{\text{V}}\text{M}^{\text{III}}(\text{PO}_4)_3$, we believe that both M^{V} and M^{III} atoms are randomly distributed in the (12c) positions of the NASICON structure. Since the structure of $\text{LiM}^{\text{V}}\text{M}^{\text{III}}(\text{PO}_4)_3$ ($\text{M}^{\text{V}} = \text{Nb, Ta}$; $\text{M}^{\text{III}} = \text{Al, Cr, Fe}$) is closely similar to that of $\text{LiTi}_2(\text{PO}_4)_3$ ¹¹ which is a good lithium-ion conductor,⁵ we expected that members of $\text{LiM}^{\text{V}}\text{M}^{\text{III}}(\text{PO}_4)_3$ would also exhibit similar lithium-ion conduction.

Fig. 4 shows the Arrhenius plots for the lithium-ion conductivity of $\text{LiM}^{\text{V}}\text{M}^{\text{III}}(\text{PO}_4)_3$ members and in Table 1, conductivity values at room temperature and at $350\text{ }^\circ\text{C}$ are given together with activation energy (E_a) values. We see that, between $\text{Nb}^{\text{V}}\text{M}^{\text{III}}$ and $\text{Ta}^{\text{V}}\text{M}^{\text{III}}$ members, the $\text{Ta}^{\text{V}}\text{M}^{\text{III}}$ members show a higher conductivity. Among the Ta^{V} -containing members, the TaAl -compound, $\text{LiTaAl}(\text{PO}_4)_3$ which has the smallest cell volume (1315 Å^3) shows the highest total ionic (bulk + grain boundary) conductivity ($\sigma_{\text{total}} = 6.5 \times 10^{-7} \text{ S cm}^{-1}$ at $30\text{ }^\circ\text{C}$ and

$\sigma_{\text{total}} = 1.0 \times 10^{-2} \text{ S cm}^{-1}$ at 350°C) with the lowest $E_a = 0.47 \text{ eV}$. From a comparison of the corresponding literature data for $\text{LiTi}_2(\text{PO}_4)_3$ (Table 1), we see that the conductivity of $\text{LiTaAl}(\text{PO}_4)_3$ is indeed higher than that of $\text{LiTi}_2(\text{PO}_4)_3$ at higher temperatures (at 350°C , for example, σ_{total} for $\text{LiTaAl}(\text{PO}_4)_3$ is $1.0 \times 10^{-2} \text{ S cm}^{-1}$ and σ_{total} for $\text{LiTi}_2(\text{PO}_4)_3$ is $6.3 \times 10^{-3} \text{ S cm}^{-1}$), albeit the activation energy for conduction of $\text{LiTaAl}(\text{PO}_4)_3$ ($E_a = 0.47 \text{ eV}$) is higher than that for $\text{LiTi}_2(\text{PO}_4)_3$ ($E_a \approx 0.30 \text{ eV}$). In the literature,⁴ a correlation between unit cell volume (V) of NASICON phosphates and activation energy, E_a , has been pointed out; E_a has been found to be a minimum (ca. 0.30 eV) when $V = 1310 \text{ \AA}^3$, corresponding to that of $\text{LiTi}_2(\text{PO}_4)_3$.

Among the $\text{LiM}^{\text{V}}\text{M}^{\text{III}}(\text{PO}_4)_3$ investigated here, $\text{LiTaAl}(\text{PO}_4)_3$ has the smallest $V = 1315 \text{ \AA}^3$ and the E_a for this phase also happens to be the smallest (ca. 0.47 eV), although this value is considerably higher than that of $\text{LiTi}_2(\text{PO}_4)_3$. This observation reveals that, while the activation energy for lithium-ion migration depends on the cell volume (optimal tunnel size), it also depends on the identity of M atoms constituting the $\text{M}_2(\text{PO}_4)_3$ framework.

Having identified a NASICON-phosphate, $\text{LiTaAl}(\text{PO}_4)_3$, that exhibits a lithium-ion conduction comparable to that of $\text{LiTi}_2(\text{PO}_4)_3$, but does not contain titanium(IV), we investigated the possibility of increasing its conductivity by appropriate substitution similar to that of $\text{Li}_{1+x}\text{Ti}_{2-x}\text{Al}_x(\text{PO}_4)_3$.^{5,12} For this purpose, we prepared the composition $\text{Li}_{1.2}\text{Ta}_{0.9}\text{Al}_{1.1}(\text{PO}_4)_3$ and investigated its ionic conductivity. We find that the conductivity of this phase is nearly the same as the parent $\text{LiTaAl}(\text{PO}_4)_3$ (Fig. 4); at high temperatures (350°C), the conductivity and activation energy of $\text{Li}_{1.2}\text{Ta}_{0.9}\text{Al}_{1.1}(\text{PO}_4)_3$ tend to become slightly higher than the corresponding values of the parent phosphate (Table 1). Clearly, further work is required to understand the sinterability, porosity and ionic conductivity of $\text{Li}_{1+2x}\text{Ta}_{1-x}\text{Al}_{1+x}(\text{PO}_4)_3$ system.

In conclusion, we have identified a new lithium-ion conducting NASICON phosphate, $\text{LiTaAl}(\text{PO}_4)_3$, that exhibits a conductivity behaviour comparable to that of $\text{LiTi}_2(\text{PO}_4)_3$ —the best lithium-ion conductor among $\text{LiM}^{\text{IV}}_2(\text{PO}_4)_3$. Unlike $\text{LiTi}_2(\text{PO}_4)_3$, however, the new phosphate $\text{LiTaAl}(\text{PO}_4)_3$ containing stable Ta^{V} and Al^{III} valence states would not undergo a reduction in contact with lithium at elevated temperatures and, accordingly, the material deserves further attention towards tailoring electrolyte materials for solid-state lithium batteries.

Acknowledgements

We thank the Indo-French Centre for the Promotion of Advanced Research, New Delhi (Project No. 1308–03) and the Department of Science and Technology, Government of India (Project No. SP/S1/H-17/97) for financial support. J. G. thanks Professor M. Tournoux, IMN, Nantes, France for encouragement and support.

References

- 1 See, for example: C. A. Vincent and B. Scrosati, *Modern Batteries: An Introduction to Electrochemical Power Sources*, Arnold, London, 2nd edn., 1997.
- 2 F. Croce, G. B. Appetecchi, L. Persi and B. Scrosati, *Nature*, 1998, **394**, 456.
- 3 A. D. Robertson, A. R. West and A. G. Ritchie, *Solid State Ionics*, 1997, **104**, 1.
- 4 H. Aono, N. Imanaka and G. Adachi, *Acc. Chem. Res.*, 1994, **27**, 265; G. Adachi, N. Imanaka and H. Aono, *Adv. Mater.*, 1996, **8**, 127.
- 5 H. Aono, E. Sugimoto, Y. Sadaoka and G. Adachi, *J. Electrochem. Soc.*, 1989, **136**, 590; H. Aono, E. Sugimoto, Y. Sadaoka, N. Imanaka and G. Adachi, *J. Electrochem. Soc.*, 1990, **137**, 1023.
- 6 K. Kasthuri Rangan and J. Gopalakrishnan, *Inorg. Chem.*, 1995, **34**, 1969.
- 7 B. E. Taylor, A. D. English and T. Berzins, *Mater. Res. Bull.*, 1977, **12**, 171; B. V. R. Chowdari, K. Radhakrishnan, K. A. Thomas and G. V. Subba Rao, *Mater. Res. Bull.*, 1989, **24**, 221.
- 8 A. Martínez-Juárez, J. M. Rojo, J. E. Iglesias and J. Sanz, *Chem. Mater.*, 1995, **7**, 1857.
- 9 M. A. París, A. Martínez-Juárez, J. E. Iglesias, J. M. Rojo and J. Sanz, *Chem. Mater.* 1997, **9**, 1430.
- 10 L. Hagman and P. Kierkegaard, *Acta. Chem. Scand.*, 1968, **22**, 1822; H. Y. P. Hong, *Mater. Res. Bull.*, 1976, **11**, 173.
- 11 D. Tran Qui, S. Hamdoune, J. L. Soubeyroux and E. Prince, *J. Solid State Chem.*, 1988, **72**, 309; D. Petit, Ph. Colomban, G. Collin and J. P. Boilot, *Mater. Res. Bull.*, 1986, **21**, 365.
- 12 H. Aono, E. Sugimoto, Y. Sadaoka, N. Imanaka and G. Adachi, *Solid State Ionics*, 1990, **40/41**, 38.
- 13 H. Aono, E. Sugimoto, Y. Sadaoka, N. Imanaka and G. Adachi, *J. Electrochem. Soc.*, 1993, **140**, 1827.
- 14 H. Aono, E. Sugimoto, Y. Sadaoka, N. Imanaka and G. Adachi, *Solid State Ionics*, 1991, **47**, 257.
- 15 F. Sudreau, D. Petit and J. P. Boilot, *J. Solid State Chem.*, 1989, **83**, 78; M. Casciola, V. Costantino, L. Merlini, I. G. K. Andersen and E. K. Andersen, *Solid State Ionics*, 1988, **26**, 229.

Paper 8/07007E